F70 - mechanics and vacuum

Fortgeschrittenen Praktikum Universität Heidelberg

Nick Striebel

December 2020

Abstract

The goal of this experiment is to become familiar with the field of vacuum technology. In particular, the aim is to examine different types of pumps and their properties. In addition, the conductance of pipes and orifices is investigated and the common problem of leak detection is addressed.

Contents

1 Basics

1.1 Pumps

There are a lot of different vacuum pumps. The (today) most important ones are listed here.

1.1.1 Rotary vane pump

The **rotary vane pump** works using the displacing principle. The pump is very basically a cylinder with an eccentric rotor in the inside. Rotor slots are gliding on the inner wall of the cylinder. While rotating past the suction point the space between rotor and housing becomes bigger and the suction effects sets in. While the rotation continues, the cavity becomes smaller again, due to the eccentric position of the rotor. Consequently the gas gets compressed again and gets pressed out of the pump on the outlet. In the phase of compression it can happen, that for example water vapour becomes liquid due to the high pressure in the chamber. To counteract this, you can connect a gas ballast to the pump so that the pressure does not gets too high. In the experiments such a rotary vane pump is used. The **liquid ring pump** works

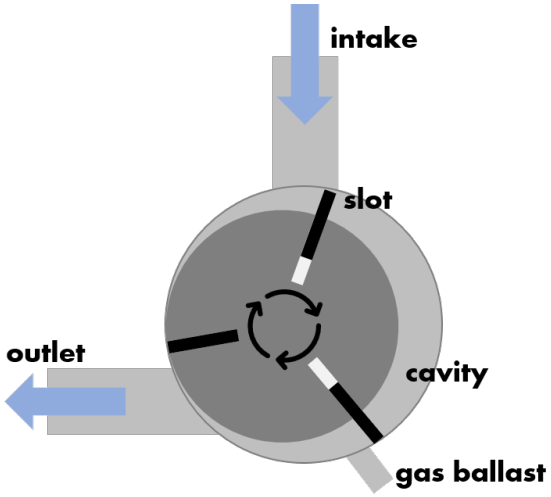

Figure 1.1: schematic structure of a rotary vane pump (inspired by [Jou18, p. 346])

similar, but instead of slidable slots the volume of the chamber changes as it is coated with a liquid.

1.1.2 Roots pump

The **Roots pump** is a pump with two rotors in it. The pump works like the rotary vane pump with the displacing principle. Two pistons shaped like eights are rotating in opposite directions. Due to the arrangement between the parts, different volumes in the chamber are created which leads to the pumping effect. The two pistons and the wall of the chamber are not touching each other, but the gaps are so small that a dynamic seal is created.

1.1.3 Oil diffusion pump

The **oil diffusion pump** uses oil as a medium to transport the gas to be pumped. On the bottom of the pump the gas is vaporized and rises in the pump. At the top the gas gets deflected to the cooled walls of the pump. Incoming molecules of the pumped gas gets caught by the oil.

The steam condensates on the walls and flows back to the bottom. Here the oil separates from the gas and the gas can be pumped of by a another pump (for example a rotary vane pump).

1.1.4 Turbo molecular pump

The most used pump for generating high vacuums is the **turbo molecular pump (TMP)**. It works with multiple rotor blades that are rotating faster than the velocity of the molecules of the pumped gas. Tu to the high speed of the rotor blades the incoming molecules receive an impulse towards the outlet of the pump. In front of the TMP a backing pump is needed. Otherwise the pressure in the chamber would damage the components of the pump.

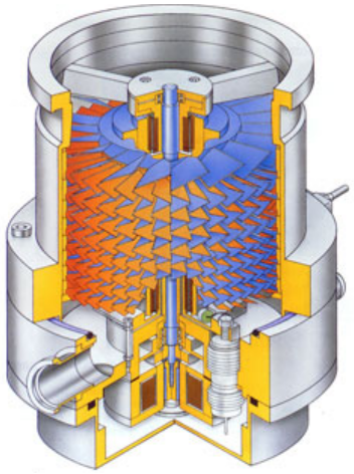

Figure 1.2: Cross section of a TMP [Cel]

1.2 Gauges

Not only for the experiment but also for the all day use gauges that measure the pressure in the vacuum chamber are essential. In this section some gauges are presented.

1.2.1 Mechanical gauges

There are a lot of different mechanical vacuum gauges but in principle they all work very similar: Either the pressure causes a shift of a component or deformation occurs. Depending on the exact type of the gauge the pressure can be determined making usage of the physical properties of the components. An advantage of these gauges is, that the pressure can be measured independent of the type of gas.
One example is the **capsule manometer**. In this case the pressure sensing element is a capsule, which will change its shape dependent on the pressure.

1.2.2 Pirani gauge

The **Pirani pump** is an gauge that that makes use of the fact, that the specific thermal conductivity of an gas is pressure-dependent. A heating wire in the inside of the vacuum chamber gets heated and the dissipated power is observed. Knowing the geometric properties and the composition of the wire the pressure in the chamber can be calculated. Today's Pirani manometers are cheap and a digital read out is possible, so these type of gauges is widespread.

1.2.3 Cold and hot cathode vacuum gauge

The **cold cathode vacuum gauge** generates an electric field by applying a voltage between the cathode and the anode. This electric field accelerates electrons which ionize the molecules of the gas. The lower the pressure the smaller the count of molecules and therefore the discharge current is smaller.
The **hot cathode vacuum gauge** works in the same way, but generates and accelerate the electrons active at the hot cathode. The electrons ionize the molecules that are left in the chamber. As before the number of molecules left in the chamber is proportional to discharge current.

2 Measurements and evaluation

The used formulas are taken from [For20]. It should be mentioned, that the lab was done online.

2.1 Pumping condensible vapours

In the first part of the experiment the pumping of water steam was examinded. With a few millilitres of water in the recipient the pumping process was started using a rotary vane pump (without a gas ballast). The observations were as follows:

1. Pumping with out the gas ballast the pressure could be reduced to 7.0 mbar
2. After attaching the gas ballast a pressure of 5.3 mbar was reached
3. At the beginning of the pumping process the water in the recipient was liquid, during the pumping process it became gaseous. After pulling it out of the recipient it was frozen.

Explanation: Pumping the water steam without the gas ballast, the pressure in the chamber inside the rotary vane pump becomes to high and the steam liquefies in the compression phase. By attaching the gas ballast the pump receives and exchanges air from the outside and the liquefaction is prevented. Thus the steam can be pumped again and a lower pressure can be achieved.
To understand the changing aggregate states of the water it is helpful to take a look at the phase diagram. Starting at standard pressure and room temperature the water is liquid (1). By reducing the pressure the water begins to evaporate (2) after passing the phase boundary. For this process evaporation heat is needed, which reduces the energy in the system and the temperature falls. While the pressure is falling the state moves close to the phase boundary. If the pressure increases again (removing the recipient from the pump) the water re-sublimates to ice (3).

2.2 Suction capacity of the Turbo molecular pump

The next goal was to measure the suction power of the TMP. For this two different methods are used. One time the pumped volume is measured by observe a small drop of soapy water in a capillary. The other time (better for high pressure) a piston prober is used. The measured values are shown in tables (2.1) and (2.2).
Unfortunately we received the data with out errors. This makes the comparison of the results harder. With the measured data we can calculate the pumping speed as follows: First the

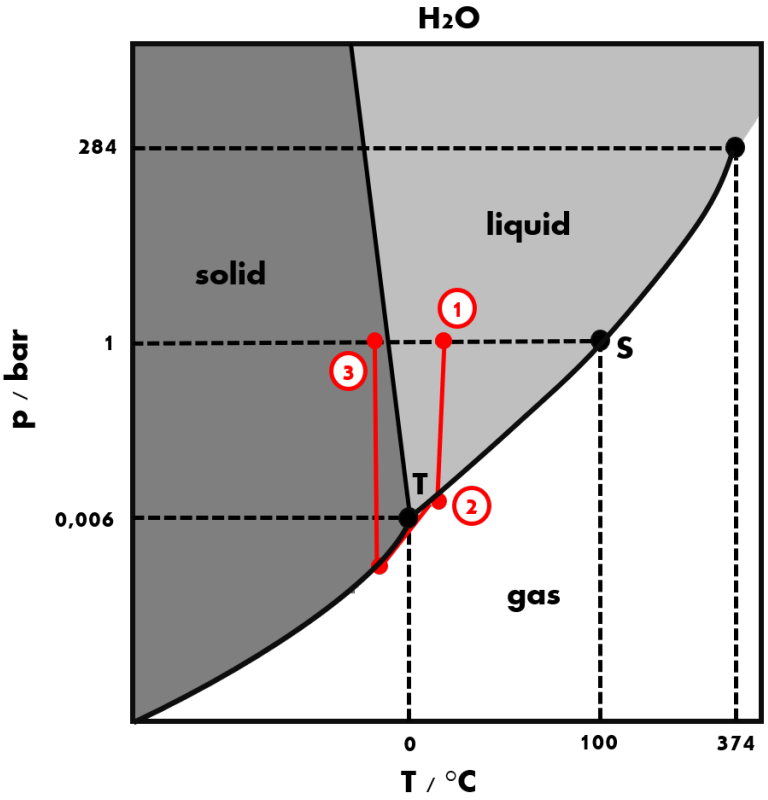

Figure 2.1: phase diagram (H_2O) according to [Hei17, p. 222]

pressure [mbar]	position 1 [ml]	position 2 [ml]	time [s]
$1.0 \cdot 10^{-5}$	0.78	0.68	338
$3.3 \cdot 10^{-5}$	0.90	0.70	86
$1.0 \cdot 10^{-4}$	1.50	1.30	25.00
$3.3 \cdot 10^{-4}$	1.60	1.30	9.80
$1.0 \cdot 10^{-3}$	1.80	0.80	12.20
$3.3 \cdot 10^{-3}$	1.90	0.90	4.00

Table 2.1: pumping speed measurement - capillary

pressure [mbar]	position 1 [ml]	position 2 [ml]	time [s]
$3.3 \cdot 10^{-4}$	12.50	7.50	91
$1.0 \cdot 10^{-3}$	24.50	19.50	49
$3.3 \cdot 10^{-3}$	15.00	10.00	18.20
$1.0 \cdot 10^{-2}$	25.00	20.00	7.00
$3.3 \cdot 10^{-2}$	25.00	20.00	3.00
$1.0 \cdot 10^{-1}$	23.00	18.00	1.34

Table 2.2: pumping speed measurement - piston

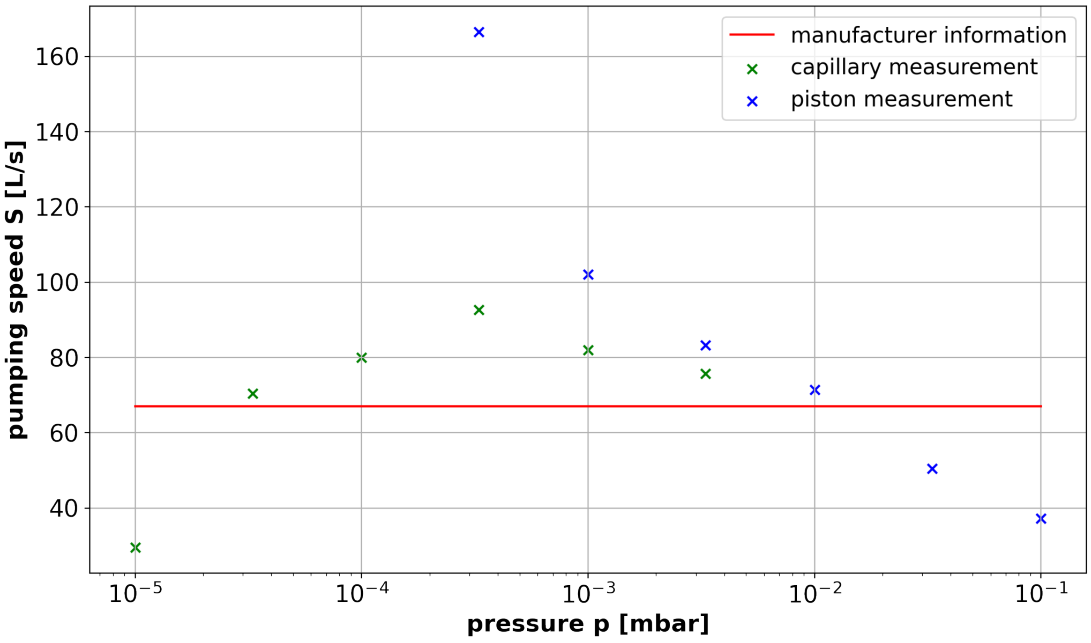

Figure 2.2: pumping speed of the TMP in dependency of the chamber pressure

change in volume ΔV_1 is calculated. Assuming, that the temperature is constant the change of volume in the recipient can be calculated using Boyle-Mariotte:

$$\frac{\Delta V_2}{\Delta V_1} = \frac{p_1}{p_2} \quad \Longleftrightarrow \quad \Delta V_2 = \frac{p_1}{p_2}\Delta V_1$$

Then the pumping speed $S = \frac{dV_a}{dt}$ can be calculated easily if we assume that in the measured time interval S is constant and one gets:

$$S_{exp} = \frac{\Delta V_2}{\Delta t}$$

Unfortunately the sticker on the pump is not completely legible and it was not possible to draw a comparison curve, but the maximum pumping speed of the *Pfeiffer HiPace 80* pumps is $67 L/s$. The results are plotted in figure (2.2). One can recognize, that the values in the middle of the pressure sequence are the closest to the manufacturer value, but in general they are to high. The piston value at $3.3 \cdot 10^{-4} mbar$ is deviating the most, probably this point comes from an incorrect measurement. For the "constant" interval between $3.3 \cdot 10^{-5}$mbar to 10^{-2}mbar the mean pumping speed is

$$S_{exp}^{mean} = (79 \pm 8)\frac{L}{s}$$

Regarding that we do not have any error values for the measurements does not makes sense to compare this value to the one of the manufacturer but the order of magnitude is the same. Additionally one can recognize that the pumping speed reduces significantly at high and low pressure values. These to flanks can be explained as follows:

- small pressure flank:
  The drop can be explainable with pseudo leaks. For very small pressure gases are leaking out of the recipient walls. Therefore the "real" pumped volume ΔV_2 (without the leaking gases) is smaller. As $S \sim \Delta V_2$ the pumping speed becomes smaller.

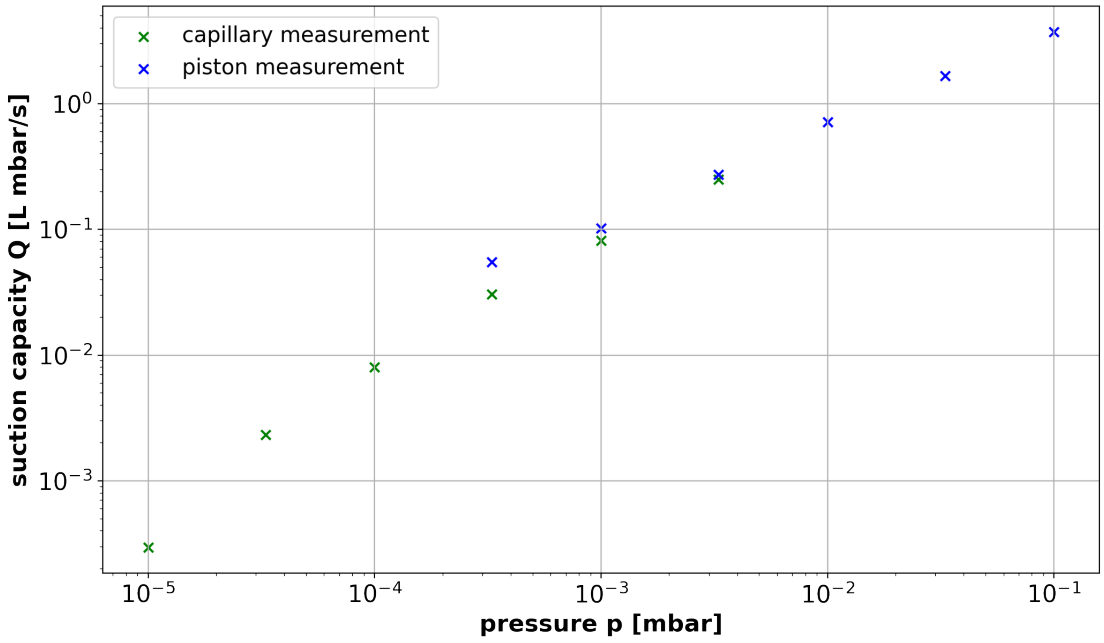

Figure 2.3: suction capacity of the TMP in dependency of the chamber pressure

- high pressure flank:
  On the other side of the pressure range the drop can be explained with the average free path length. It is to small. The TMP works by giving the molecules impulses towards the outlet of the pump. If the average free path length is to small (at higher pressures $\leftrightarrow$ more molecules) the transmitted impulses get lost in the huge number of collisions between the molecules and the TMP does not works as efficient as before.

The manufacture curve has the flank at higher pressure as well (as it is expectable due to the smaller average free mean path). The flank at small pressure does not comes up in the manufacture curve because this flank comes mainly from leaks and pseudo leaks. The manufacture assumes that one runs the TMP under perfect conditions where these leaks do not exist.
To calculate the pseudo leak rate one can regard the difference of the pumping speed S_{pseudo} at the lowest pressure p_{pseudo} and the mean pumping speed S_{mean}:

$$Q_{pseudo} = (S_{mean} - S_{pseudo}) \cdot p_{pseudo} = (5.0 \pm 0.8) \cdot 10^{-4} \frac{L \cdot mbar}{s}$$

Additionally in figure (2.3) the suction capacity ($Q = S \cdot p$) of the TMP is plotted. As expected it reduces at smaller pressure. One pays attention to the double logarithmic scale.

2.3 Conductance of tube and orifice plate

The most important part of the lab is the determination of the conductances of different connectors. For this again the TMP is used. At different levels the pressure is measured directly at the TMP (p_1) and at the end of the connector [tube/orifice plate] (p_2). The measurements are presented in the tables (2.3) to (2.5) With the experimental measured values the conductances are calculated via:

$$L_{exp} = S \cdot \frac{p_1}{p_2 - p_1}$$

S is the pumping speed. The values for S are taken from the first measurements on the TMP.

p_1 [mbar]	p_2 [mbar]	p_1 [mbar]	p_2 [mbar]
$1.20 \cdot 10^{-5}$	$1.40 \cdot 10^{-3}$	$3.70 \cdot 10^{-3}$	$1.80 \cdot 10^{-1}$
$3.60 \cdot 10^{-5}$	$4.30 \cdot 10^{-3}$	$1.10 \cdot 10^{-2}$	$2.90 \cdot 10^{-1}$
$1.10 \cdot 10^{-4}$	$1.60 \cdot 10^{-2}$	$3.60 \cdot 10^{-2}$	$4.40 \cdot 10^{-1}$
$3.60 \cdot 10^{-4}$	$3.90 \cdot 10^{-2}$	$1.60 \cdot 10^{-3}$	$1.10 \cdot 10^{-1}$
$1.10 \cdot 10^{-3}$	$9.00 \cdot 10^{-2}$	$1.10 \cdot 10^{-1}$	$7.20 \cdot 10^{-1}$

Table 2.3: conductance measurement - tube (1m length, 0.016m diameter)

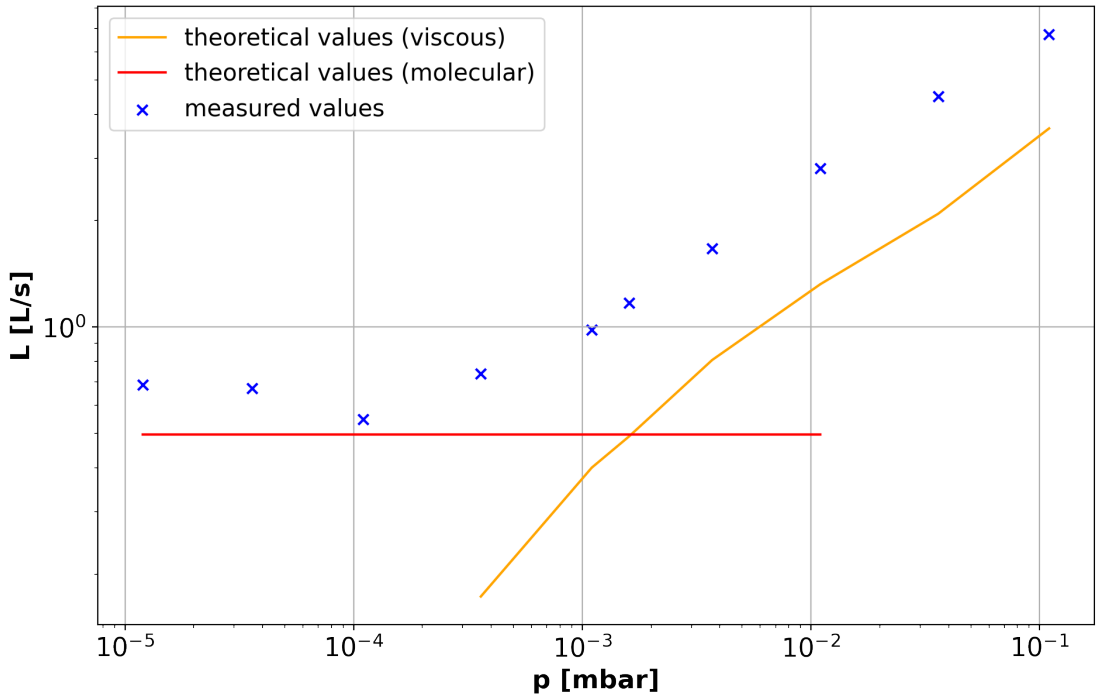

Figure 2.4: conductance of the tube in dependency of the chamber pressure

For the theoretical values for the tube are calculated with

$$L_{tube}^{theo} = \frac{\pi}{8} \cdot r^4 \cdot \frac{p_1 + p_2}{2 \cdot \eta \cdot l} \text{ (continuous flow)}$$

$$L_{tube}^{theo} = \frac{8}{3} \cdot \frac{r^3}{l} \sqrt{\frac{\pi \cdot R \cdot T}{2 \cdot M}} \text{ (molecular flow)}$$

For the orifice

$$L_{orifice}^{theo} = \frac{1}{4} \cdot \pi \cot r^2 cdot \sqrt{\frac{8}{\pi} \cdot \frac{R \cdot T}{M}}$$

is used. r is the radius of the connector, l the length, T the temperature, R the gas constant, η the viscosity of air and M the molecular mass. For the temperature we have no vlaue given, so we just assume that the room temperature was $20C$. The theoretical value for the connectors

p_1 [mbar]	p_2 [mbar]	p_1 [mbar]	p_2 [mbar]
$2.10 \cdot 10^{-5}$	$6.70 \cdot 10^{-5}$	$1.30 \cdot 10^{-4}$	$1.00 \cdot 10^{-2}$
$2.00 \cdot 10^{-5}$	$7.00 \cdot 10^{-5}$	$4.60 \cdot 10^{-4}$	$3.50 \cdot 10^{-2}$
$1.90 \cdot 10^{-5}$	$1.10 \cdot 10^{-4}$	$1.80 \cdot 10^{-3}$	$1.00 \cdot 10^{-1}$
$2.00 \cdot 10^{-5}$	$3.20 \cdot 10^{-4}$	$6.90 \cdot 10^{-3}$	$3.30 \cdot 10^{-1}$
$2.90 \cdot 10^{-5}$	$1.10 \cdot 10^{-3}$	$3.10 \cdot 10^{-2}$	1.00
$5.40 \cdot 10^{-5}$	$3.20 \cdot 10^{-3}$	$2.80 \cdot 10^{-5}$	3.40

Table 2.4: conductance measurement - orifice (0.002m thick, 0.004m diameter)

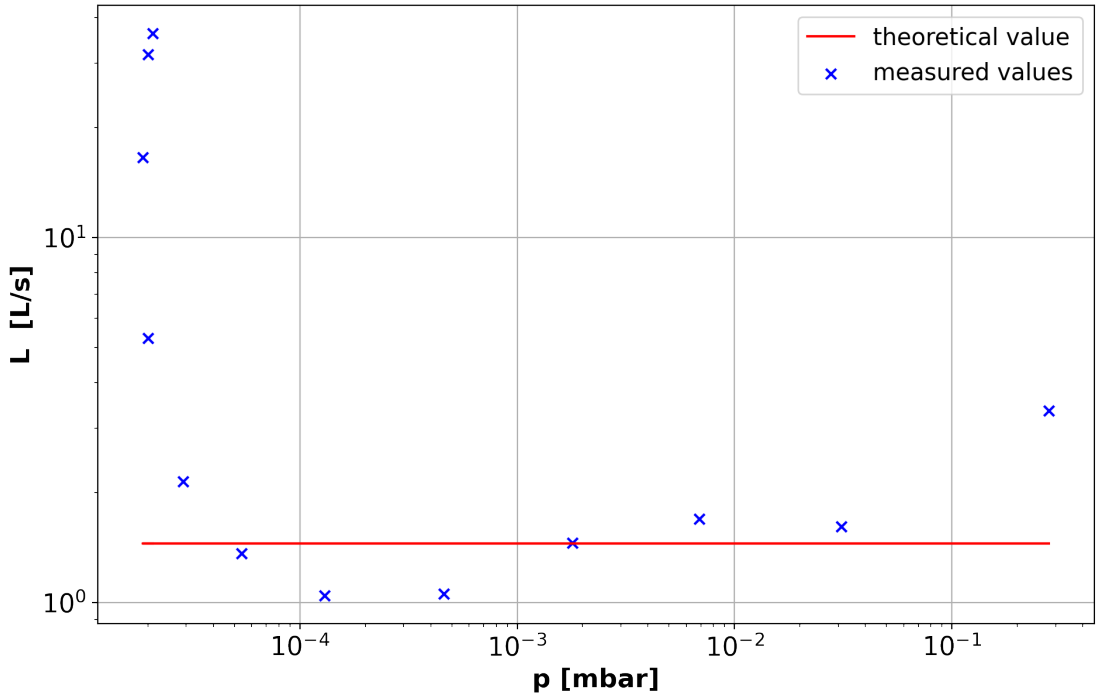

Figure 2.5: conductance of the orifice in dependency of the chamber pressure

in series are calculated using the experimental results for L and the rule of Kirchhoff for series connection:

$$\frac{1}{L_{ges}} = \frac{1}{L_1} + \frac{1}{L_2} \Rightarrow L_{ges} = \frac{1}{\frac{1}{L_1} + \frac{1}{L_2}}$$

The single measurements of tube and orifice are not done at the same pressures sometimes, so there are not so many theoretical values for the series plot. The results are plotted in figures (2.4) to (2.6).
In the tube plot one can see how measured values have the behaviour one would expect: For low pressures L is nearly constant (molecular flow). For higher pressures the points follow the formula for viscous flow. L_{exp} is deviate systematically upwards in comparison to the theoretically values. This is discussed in section (3.2).
The orifice plot shows a nice agreement of the theoretical and experimental values for pressures higher than $5 \cdot 10^{-5}$mbar. On the left a steep flank appears. This is explainable with the rising leak currents: At lower pressures pseudo leaks have a higher importance. Thus it seems like there is more volume pumped and L increases.

p_1 [mbar]	p_2 [mbar]	p_1 [mbar]	p_2 [mbar]
$1.60 \cdot 10^{-5}$	$1.50 \cdot 10^{-4}$	$1.20 \cdot 10^{-3}$	$1.30 \cdot 10^{-1}$
$1.90 \cdot 10^{-5}$	$1.10 \cdot 10^{-3}$	$3.30 \cdot 10^{-3}$	$2.70 \cdot 10^{-1}$
$3.50 \cdot 10^{-5}$	$5.30 \cdot 10^{-3}$	$1.00 \cdot 10^{-2}$	$5.50 \cdot 10^{-1}$
$1.00 \cdot 10^{-4}$	$2.20 \cdot 10^{-2}$	$3.50 \cdot 10^{-2}$	1.10
$3.70 \cdot 10^{-4}$	$6.00 \cdot 10^{-2}$	$1.40 \cdot 10^{-1}$	2.50

Table 2.5: conductance measurement - tube and orifice in series

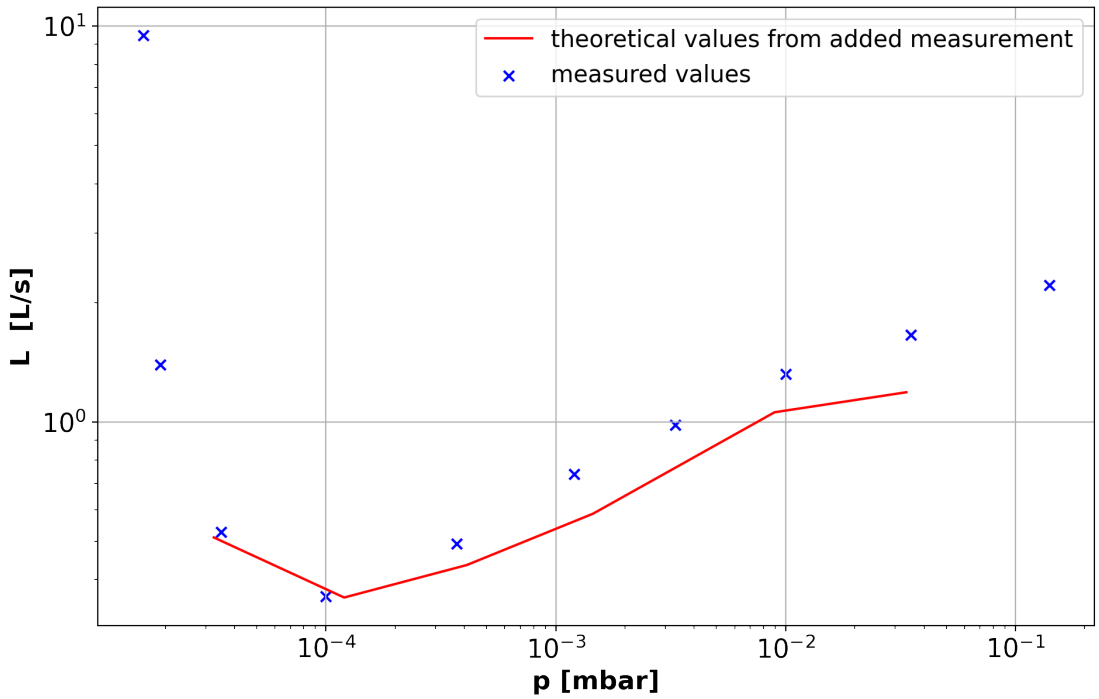

Figure 2.6: conductance of the tube and orifices in series in dependency of the chamber pressure

Do not knowing the errors of the measurements one can still says, that the series plot shows how good the rule of Kirchhoff for a series connection works: The measured and theoretical values are close.

2.4 Leak detection

Last the leak detection was handled. This part is more qualitative compared to the others.
The most sensitive method to find leaks works with helium. In this experiment a counter current leak detector is used. The working principle is very simple. One sprays Helium on the part of the object where one suspects the leak, while a high vacuum pump is pumping. The helium gas is soaked in trough the leak and reaches the mass spectrometer in the counter current and gets detected. The advantage of helium is, that it has nucleon number 4, is very small and that it is a noble gas.
If one would like to calculate the leak rate of a very small leak (in this experiment a very small hole in a glass capillary) one can assume that the pumping speed S_0 without the leak is approximately the same as the pumping speed S_1 with the leak (as seen in figure (2.2)). Let Q_0 and Q_1 be the suction capacities without and with the leak. The leak rate is than calculated via

$$Q_{leak} = Q_1 - Q_0 \approx S \cdot (p_1 - p_0)$$

where $S = S_0 \approx S_1$.

3 Discussion and Conclusion

3.1 Suction power of the TMP

The estimation of the pumping speed and suction power worked okay. The piston measurement has one big outlier but the rest of the measured data points is in the near of the theoretical value. Due to the missing errors on the measurement it is hard to rank the result correctly. Possibly error sources are the usage of Boyle-Mariotte (it assumes that the temperature is constant) and of course the measurement of the change in volume with the water drop is not the precisest one.
The two flanks at low and high pressure are expected and can be explained with pseudo leaks and the average free path length as it is done in section (2.2). Additionally the pseudo leak rate could be estimated.

3.2 Conductances

In the second part of the experiment the conductance of different connectors was analysed. The measurements on the tube showed the expected course but all experimental values are higher than the theoretical values. Possible error sources are the neglect of friction effects and deviations of from the pumping speed measurements.
Secondly the orifice was analysed. Here the experimental values (not knowing the errors of the measurement) seem to be close to the theoretical value (apart the flank at lower pressures). The flank could be explained with pseudo leaks (see section (2.3)). A possibly error source in these measurement are the assumption that the orifice plate is infinitesimal thin.
The result of the measurement where the tube and orifice were connected in series is very good. The rule of Kirchhoff is confirmed as the experimental and theoretical values agree with each other (again we do not know any errors on the data).

3.3 Summary

These experiment gives a nice intro to the world of the vacuum technology. Of course it would have been nice if we could have done the lab on site but the most important parts of the experiments were communicated. Beside the analysis of different types of pumps the conductance of different connectors and the daily problem of leaks have been addressed.

References

[Cel] Celladoor. *LHC - Vakuumtechnik*. URL: `http://www.lhc-facts.ch/index.php?page=vakuum` (visited on 12/16/2020).

[For20] Fortgeschrittenen Praktikum, ed. *FP70/71 Mechanik und Vakuum*. Universität Heidelberg, 2020.

[Hei17] Andreas Heintz. *Thermodynamik. Grundlagen und Anwendungen*. 2017.

[Jou18] Karl Jousten. *Handbuch Vakuumtechnik*. Springer, 2018.